RESEARCH REPORTS
Clinical

E.S. Cho[1], K.-J. Kim[2], K.-E. Lee[2], E.-J. Lee[2], C.Y. Yun[1], M.-J. Lee[3], T.J. Shin[2], H.-K. Hyun[2], Y.-J. Kim[2], S.-H. Lee[2], H.-S. Jung[3], Z.H. Lee[4], and J.-W. Kim[2,5]*

[1]Cluster for Craniofacial Development and Regeneration Research, Institute of Oral Biosciences, School of Dentistry, Chonbuk National University, Jeonju, Korea; [2]Department of Pediatric Dentistry and Dental Research Institute, School of Dentistry, Seoul National University, Seoul, Korea; [3]Division in Anatomy and Developmental Biology, Department of Oral Biology, College of Dentistry, Yonsei University, Seoul, Korea; [4]Department of Cell and Developmental Biology and Dental Research Institute, School of Dentistry, Seoul National University, Seoul, Korea; and [5]Department of Molecular Genetics and Dental Research Institute, School of Dentistry, Seoul National University, Seoul, Korea; *corresponding author, pedoman@snu.ac.kr

J Dent Res 93(10):980-987, 2014

Alteration of Conserved Alternative Splicing in *AMELX* Causes Enamel Defects

ABSTRACT

Tooth enamel is the most highly mineralized tissue in vertebrates. Enamel crystal formation and elongation should be well controlled to achieve an exceptional hardness and a compact microstructure. Enamel matrix calcification occurs with several matrix proteins, such as amelogenin, enamelin, and ameloblastin. Among them, amelogenin is the most abundant enamel matrix protein, and multiple isoforms resulting from extensive but well-conserved alternative splicing and postsecretional processing have been identified. In this report, we recruited a family with a unique enamel defect and identified a silent mutation in exon 4 of the *AMELX* gene. We show that the mutation caused the inclusion of exon 4, which is almost always skipped, in the mRNA transcript. We further show, by generating and characterizing a transgenic animal model, that the alteration of the ratio and quantity of the developmentally conserved alternative splicing repertoire of *AMELX* caused defects in enamel matrix mineralization.

KEY WORDS: amelogenesis imperfecta, X-linked, tooth, silent mutation, amelogenin, mRNA splicing.

DOI: 10.1177/0022034514547272

Received May 10, 2014; Last revision July 12, 2014; Accepted July 23, 2014

A supplemental appendix to this article is published electronically only at http://jdr.sagepub.com/supplemental.

INTRODUCTION

Tooth enamel is the hardest tissue in the human body. The development of tooth enamel is a result of a series of ectomesenchymal interactions (Thesleff, 1995). Once the inner enamel epithelium cells differentiate to ameloblasts, ameloblasts secrete enamel matrix proteins into the developing enamel matrix, and the enamel matrix begins to calcify. To achieve an exceptional hardness and a fine structure, the calcified enamel undergoes a maturation process.

Defects in tooth enamel can be caused by environmental as well as genetic factors. *Amelogenesis imperfecta* (AI) is a collective term referring to inherited malformation of tooth enamel. There are 3 major categories of AI: hypoplastic, hypocalcified, and hypomatured. The enamel is thin in hypoplastic AI. Hypocalcified enamel is extremely soft such that it easily abrades after tooth eruption due to the occlusal force. Hypomatured enamel is discolored and soft but has a normal thickness (Witkop, 1988).

Mutational analysis has initially focused on genes encoding enamel matrix proteins, identifying mutations in amelogenin (*AMELX*; Kim *et al.*, 2004), enamelin (*ENAM*; Kang *et al.*, 2009), kallikrein 4 (*KLK4*; Hart *et al.*, 2004) and enamelysin (*MMP20*; Kim *et al.*, 2005b). Genetic analysis—such as linkage analysis, autozygosity mapping, and exome sequencing—has recently identified mutations in the family with sequence similarity 83 member H (*FAM83H*; Kim *et al.*, 2008), WD repeat-containing protein 72 (*WDR72*; El-Sayed *et al.*, 2009; Lee *et al.*, 2010), family with sequence similarity 20 member A (*FAM20A*; O'Sullivan *et al.*, 2011; Cho *et al.*, 2012), chromosome 4 open reading frame 26 (*C4orf26*; Parry *et al.*, 2012), solute carrier family 24 member 4 (*SLC24A4*; Parry *et al.*, 2013), laminin beta 3 (*LAMB3*; Kim *et al.*, 2013; Poulter *et al.*, 2014b), and integrin beta 6 (*ITGB6*; Poulter *et al.*, 2014a; Wang *et al.*, 2014).

Amelogenin constitutes up to 90% of the protein in the developing enamel matrix, and only a thin layer of enamel is formed in *AmelX* knockout mice (Gibson *et al.*, 2001). Extensive alternative splicing of the amelogenin primary RNA transcript is a general feature of amelogenin biosynthesis. Exon skipping and utilization of alternative 3′ splicing acceptor sites in exons

explain the mechanism behind amelogenin mRNA diversity (Gibson, 1999). While the murine amelogenin gene is on the X chromosome, the human amelogenin genes are located on both the X (*AMELX*, OMIM *300391) and Y (*AMELY*, OMIM *410000) chromosomes. Both genes do not equally contribute to the pool of amelogenin, with *AMELY*-derived mRNA accounting for only 10% of the total amelogenin transcripts (Salido *et al.*, 1992). The human *AMELX* gene has 7 exons, and translation begins in exon 2. Exon 4, encoding 14 amino acids, is almost always skipped during pre-mRNA splicing, so the full-length mRNA containing exon 4 is not the major transcript. The most abundant mRNA is an exon 4 skipped full-length transcript (Salido *et al.*, 1992).

The functional importance of amelogenin and its isoforms during enamel formation has been extensively studied; however, the effect of including exon 4 in amelogenesis remains unknown. In this study, we identified a family with a unique AI clinical phenotype and found a single-nucleotide transition in exon 4 of the *AMELX* gene, which altered the developmentally conserved splicing repertoire causing the inclusion of exon 4. We generated transgenic mice overexpressing full-length amelogenin that included exon 4 and characterized it to identify the effect of including exon 4 in amelogenesis.

MATERIALS & METHODS

Ethics Statement

The human study protocol and patient consent were reviewed and approved by the Institution Review Board at Seoul National University Dental Hospital. Blood samples were collected with the understanding and written consent of each participant according to the Declaration of Helsinki. All procedures involving transgenic animals were reviewed and approved by the Seoul National University Institutional Animal Care and Use Committee.

Mutational and Linkage Analyses

Mutational analyses including exons and nearby intron sequences were done for the *AMELX* gene, using DNA samples of the affected mother (V:6), based on the candidate gene approach (Fig. 1A). The primer pairs and polymerase chain reaction (PCR) conditions were described previously (Kim *et al.*, 2004). After sequencing of the *AMELX* gene, other candidate genes were sequenced as described elsewhere (Kim *et al.*, 2005a; Kim *et al.*, 2006; Appendix Table 1). Primers for the *AMTN* and *ODAM* genes were designed with Primer3 (http://frodo.wi.mit.edu/primer3/). Linkage analysis was performed with STR (short tandem repeat) markers for known genes (Appendix Table 2). After the linkage analysis (Appendix Table 3), all introns and the promoter region (1.5 kb) of *AMELX* were sequenced (Appendix Table 4).

Splicing Assay

A fragment (736 bp) of the *AMELX* gene including exons 4 and 5 was amplified with the Pfu enzyme (Elpis biotech, Taejeon, Korea) and cloned into the pSPL3 vector after double digestion with *Eco*RI and *Bam*HI restriction endonucleases (Appendix Table 5). Cloned vectors were transfected into COS-7 cells, and total RNA was isolated after 36 hr. Reverse transcriptase PCR was performed with vector primers (SD6: 5′-TCTGAGTCAC CTGGACAACC-3′, SA2: 5′-ATCTCAGTGGTATTTGTG AGC-3′). Amplification bands were excised from an agarose gel and characterized by sequencing. The entire *AMELX* gene including all 7 exons was also cloned into the pSPL3 vector (Appendix Table 5). The anterior part of the *AMELX* gene (exons 1-5) was amplified and cloned with *Eco*RI and *Not*I restriction endonucleases. The posterior part (exons 4-7) was cloned into the vector *via Kpn*I and *Not*I. Transfection and total RNA isolation were performed as described above. Reverse transcriptase PCR was performed with exon-specific primers (sense: 5′-CAAGCATCCCTGAGTTTCAA-3′, antisense: 5′-C CCCTCTCATCTTCTGATCTTTT-3′). Amplification bands were excised from a polyacrylamide gel and cloned through the Topcloner PCR cloning kit (Enzynomics, Seoul, Korea). Multiple clones from each band were sequenced and characterized.

Generation of Transgenic Mice

The mouse *Amelx* vector (Chun *et al.*, 2010) was used for tissue-specific expression of the mouse full-length amelogenin including exon 4 (M194). The cDNA was amplified and cloned into the vector after digestion with *Asc*I and *Sgf*I restriction endonucleases (Appendix Table 6). The small additional sequence (11 bp) from the ligation in exon 2 was removed by PCR mutagenesis (11bp_rem). The 6.4-kb transgene was excised from the vector by restriction digestion with *Not*I-*Srf*I and used to generate transgenic C57BL/6N mice (Macrogen, Seoul, Korea).

RESULTS

Recruitment of AI Family

The proband was a 9.5-year-old girl in a nonconsanguineous family (Fig. 1A), presenting generalized pitted hypoplastic AI with spotted brown pigmentation (Fig. 1B-1E). Clinical examination of the affected mother and brother revealed that the phenotype was largely hypomaturation with some pitted hypoplastic regions (Fig. 1F; Appendix Fig. 1). The enamel was less mineralized based on reduced contrast between the enamel and dentin (Fig. 1G and 1H). Patients had some thermal sensitivity, but the severity was reported to be mild. Pedigree analysis suggested an X-linked inheritance pattern (Fig. 1A).

Identification of a Silent Mutation in the *AMELX* Gene

Candidate gene sequencing of exons and exon-intron boundaries of the *AMELX* gene revealed a synonymous variation in exon 4 (NM_182680.1; c.120T>C, p.Ala40Ala; Fig. 2A). The 6 affected persons had this sequence variation, and none of the 7 unaffected persons had it. This nucleotide change was well conserved in all species except for the opossum (Sire *et al.*, 2012). Further sequencing of the other AI-related genes did not identify any disease-causing mutations. Linkage analysis was performed

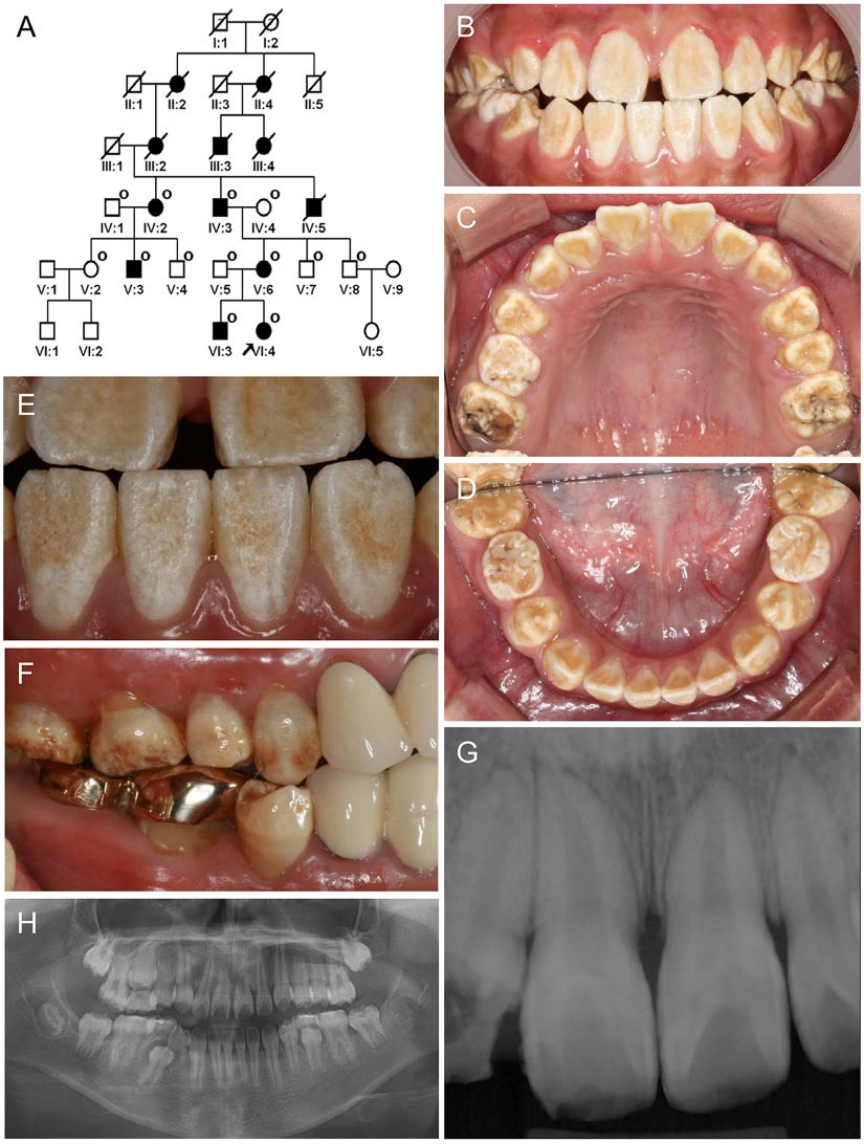

Figure 1. Pedigree, clinical photographs, and dental radiographs of the affected individuals. (**A**) Pedigree of the family. Arrow indicates the proband, and the symbol O indicates family members who participated in the study. (**B-E**) Frontal, maxillary, and mandibular clinical photographs of the proband. Teeth have a generalized pitted hypoplastic enamel with spotted brown pigmentation. (**F**) A buccal clinical photograph of the mother of the proband (V6). Hypoplastic as well as hypomineralized enamel is evident. (**G**) Intraoral radiograph of the brother of the proband (VI3) revealed a reduced contrast between the enamel and dentin due to the diminished mineral density of the affected enamel. (**H**) Panoramic radiograph of the proband showed a reduced enamel thickness and density.

with participating family members (6 affected and 7 unaffected) and confirmed that *AMELX* was the only gene linked to the AI in this family (Figure 1A, Appendix Table 3). The introns and the promoter region of the *AMELX* gene were also sequenced, but no other pathologic variation was identified. The only sequence variation identified in the introns and the promoter region was an intronic variation with minor allele frequency of 0.300 (rs946252; c.54+65T>C in the intron 2), and this variation was ruled out as a disease-causing variation based on its allele frequency.

Effect of the Silent Mutation on Pre-mRNA Splicing

Minigene splicing assay including exons 4 and 5 revealed that exon 4 was almost skipped in the wild type, whereas exon 4 was more frequently included than skipped in the mutant construct (Fig. 2B). Splicing assay of the whole *AMELX* gene identified alternative splicing products (Fig. 2C). An internal splicing site in exon 6 was identified as well, and the internal splicing product included only the 3′ 75 bp instead of the entire exon 6 (426 bp). The wild-type allele resulted in 6 alternative splicing products, and the mutant allele resulted in 2 additional splicing products.

Phenotypic Analysis of Exfoliated Deciduous Mandibular Second Molars

The exfoliated deciduous mandibular second molars from the proband showed localized pitted enamel surfaces (Fig. 3A, 3B). Micro–computed tomography (microCT) image analysis showed reduced radiodensity of the affected enamel compared with the wild type, indicating that the affected enamel was less mineralized (Fig. 3C, 3D). Scanning electron microscopic (SEM) examination of the external surface of the affected tooth confirmed hypoplastic pits (Fig. 3E-3G), and SEM examination of the cross-sectional surface showed atypical enamel structures with some normal-looking enamel structures (Fig. 3H). Normal-looking enamel was located near the dentinoenamel junction. Higher magnifications of the normal-looking enamel region revealed well-organized enamel prisms (Fig. 3I1-3I3). Atypical enamel structures were observed in all the other areas. Higher magnifications of an atypical area revealed an irregular shape of the enamel prisms (Fig. 3J1-3J3). Another atypical area showed crater-shaped voids and an amorphous shape of the enamel prisms (Fig. 3K1-3K3). The enamel structure of the wild-type tooth was well organized and uniform throughout the entire enamel thickness (Fig. 3L). Higher magnifications revealed closely packed well-organized enamel prisms (Fig. 3L1-3L3).

Macroscopic and Microscopic Analyses of Transgenic Mice

Two lines of transgenic mice overexpressing M194 were analyzed. The anterior teeth of the transgenic mice looked whiter compared with the brown teeth of the wild-type animal (Fig. 4A-4H). The molar teeth were severely worn such that the pulp tissue could be seen through the thin coverage. A histologic section of the mandibular anterior tooth showed that the enamel layer was less mineralized and thinner than that of the wild-type enamel layer (Fig. 4I1-4J6). The affected enamel layer contained irregular mineralized regions, and the enamel surface was not as smooth as the wild-type enamel. The ameloblasts were not well organized, especially in the maturation stages (Fig. 4J5, 4J6). Antiamelogenin antibody staining showed a reduction in amelogenin expression and secretion after the late-secretory stage in the transgenic mice (Fig. 4K1-4L6).

SEM and MicroCT Analysis of the Transgenic Mice

The hypomineralized enamel of the transgenic mice was so weak that the enamel surface was irregular and thin after extraction (Appendix Fig. 2A). The affected enamel layer showed an irregular enamel structure with an amorphous calcification pattern with numerous pores (Appendix Fig. 2B-2D). The extracted teeth showed irregular and less mineralized enamel with an eroded surface after teeth eruption, compared to sound mineralized enamel with the luster of the wild-type anterior tooth (Appendix Fig. 2E-2G). SEM image of the wild-type mouse showed well-organized enamel prisms (Appendix Fig. 2H). MicroCT image analysis revealed that the affected enamel had a reduced enamel density, resembling no enamel coverage (Appendix Fig. 2I-2L).

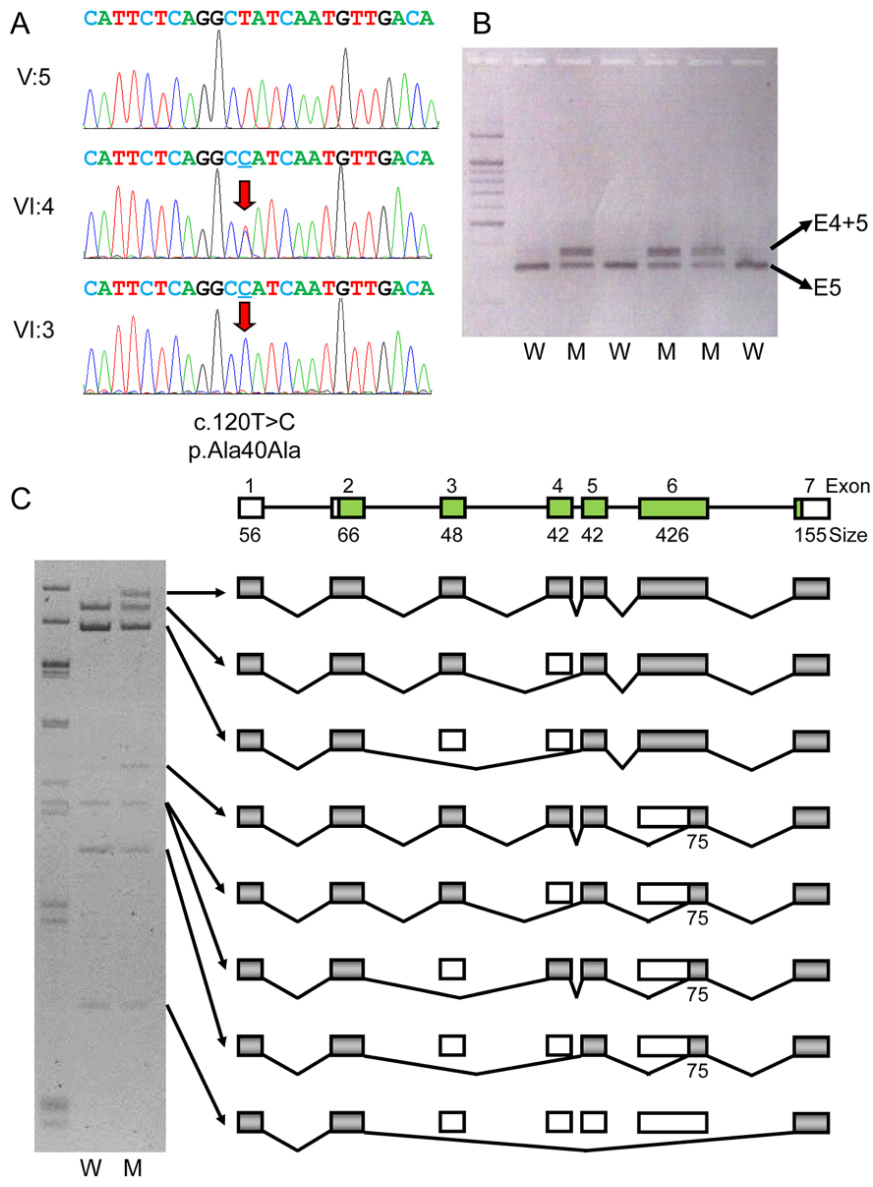

Figure 2. Mutational analysis and splicing assay. (**A**) Sanger sequencing chromatograms of the unaffected father (V5), the proband (VI4), and the brother of the proband (VI3). Red arrows indicate mutated nucleotide position, and the mutated nucleotide is indicated by the underline. (**B**) Minigene splicing assay of the revealed mutation resulted in the inclusion of exon 4 in the mRNA transcript. (**C**) Whole gene splicing assay. Normal gene diagram is shown on the top. The numbers above the boxes (exons) indicate the exon numbers, and the numbers under the boxes indicate the nucleotide length of the exon. Green areas indicate coding exons. Resulting mRNA transcripts from each band of the PAGE gel are shown as splicing diagrams. W denotes wild type and M denotes mutated clone. Left lane is a DNA marker.

DISCUSSION

Synonymous changes in the nucleotide sequence were, until recently, considered neutral or silent. It has been shown, however, that silent mutations can cause diseases by affecting pre-mRNA splicing, mRNA stability, and protein synthesis rates through codon usage bias (Sauna and Kimchi-Sarfaty, 2011). In this report, we confirmed that a silent mutation (c.120T>C, p.Ala40Ala) increased the exon definition, resulting in the inclusion of exon 4, which is almost always skipped in the wild-type *AMELX* splicing mRNA transcripts.

Sequence analysis based on Human Splicing Finder (http://www.umd.be/HSF/) showed changes in motif scores in exonic splicing enhancer as well as exonic splicing silencer (ESS) (Desmet *et al.*, 2009). The binding score of the SC35 (SRSF2; serine/arginine-rich splicing factor 2), one of the exonic splicing

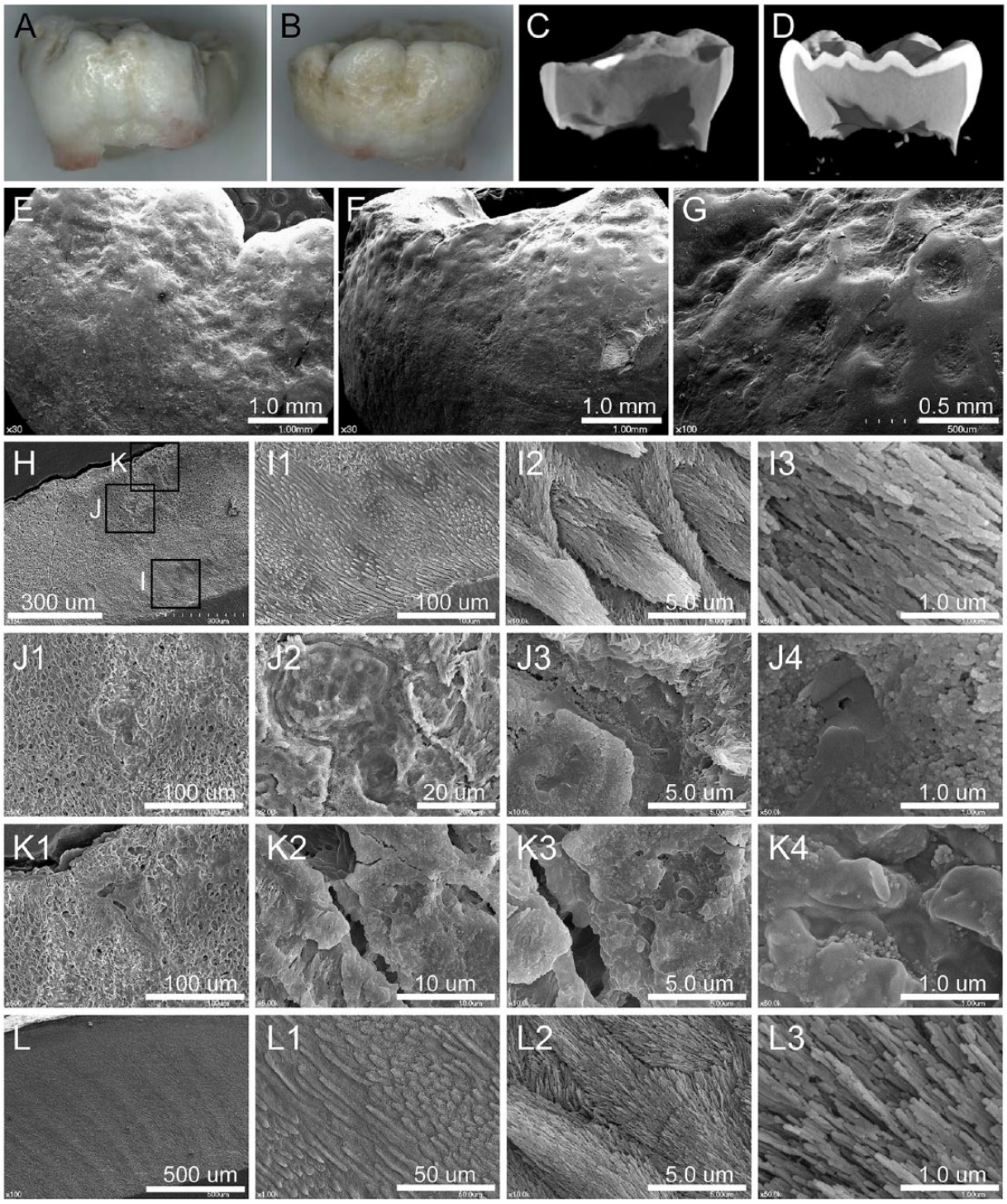

Figure 3. Phenotypic analysis of exfoliated deciduous mandibular second molars of the proband. (**A, B**) Clinical photographs of an exfoliated deciduous mandibular second molar: lingual (A) and buccal view (B). (**C, D**) Micro–computed tomography images of an exfoliated deciduous mandibular second molar of the proband (C) and a healthy individual (D). Reduced enamel density is evident in the affected tooth compared with a wild-type one. (**E-G**) Scanning electron microscopic (SEM) images of the surface of the affected tooth. (**H**) Cross-sectional SEM image of the affected tooth. (**I-K**) Three areas with higher magnification are indicated as black boxes. (**I1-I3**) Normal-looking area in the affected tooth. Normal crystal structure is observed in a series of higher magnifications. (**J1-J3**) Higher magnifications of an atypical area reveal the irregular shape of the enamel prisms. (**K1-K3**) Another atypical area shows numerous voids and the amorphous shape of the enamel prisms. (**L**) Cross-sectional SEM image of a wild-type tooth. Enamel structure is well organized and uniform throughout the entire enamel thickness. (**L1-L3**) Higher magnifications reveal closely packed well-organized enamel prisms. Length of bar is indicated above the bar.

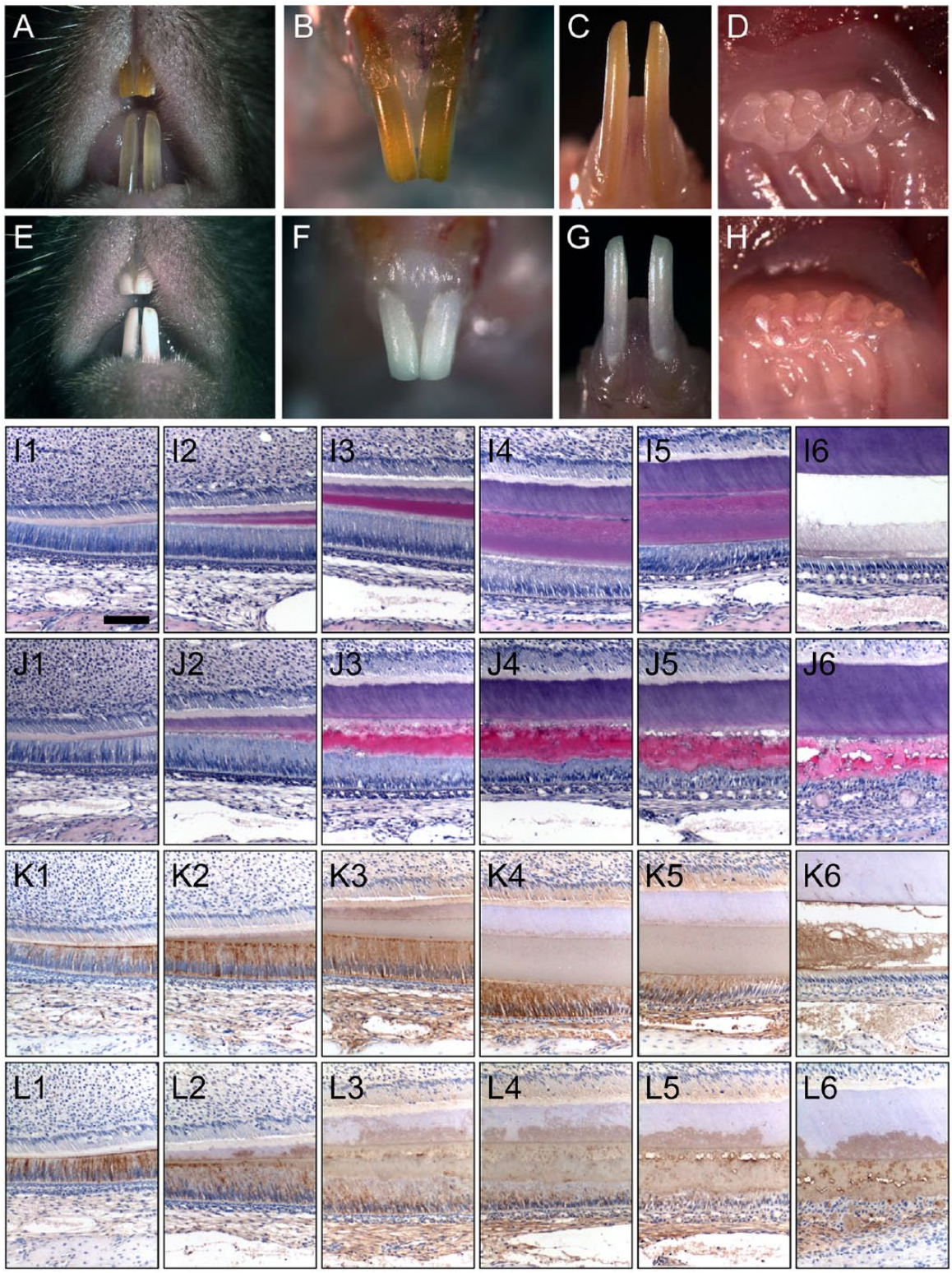

Figure 4. Phenotypic and immunohistologic analysis of the transgenic mice. (**A-D**) Photos of wild-type mouse: anterior image (A), maxillary anterior teeth (B), mandibular anterior teeth (C), and maxillary posterior teeth (D). (**E-H**) Photos of a transgenic mouse: anterior image (E), maxillary anterior teeth (F), mandibular anterior teeth (G), and maxillary posterior teeth (H). Teeth of the transgenic mouse are whiter than the wild type, and the occlusal surfaces are eroded down to the gingival level. (**I1-I6**) Series of images of the mandibular anterior tooth of the wild-type mouse stained with hematoxylin and eosin. (**J1-J6**) Series of images of the mandibular anterior tooth of the transgenic mouse stained with hematoxylin and eosin. (**K1-K6**) Series of images of the mandibular anterior tooth of the wild-type mouse stained with antiamelogenin antibody. (**L1-L6**) Series of images of the mandibular anterior tooth of the transgenic mouse stained with antiamelogenin antibody. Scale bar indicates 100 μm.

enhancer proteins, increased to 79.84 with the mutation (GGCTATCA) from 78.43 seen in the wild type (GGCCATCA). Additionally, the motif 3 of the ESS (GCTATCAA) changed to undetectable with conventional threshold values of 60, from scores of 63.50 seen in the wild type. Therefore, the analysis revealed that the increased exon definition caused by the mutation occurred by both the reinforcement of the binding of SC35 and the weakening of an ESS binding.

The amelogenin coding gene is, in general, composed of 7 exons in mammals, but there are 2 additional exons in the rat and mouse. Among them, cDNA transcripts including exon 4 are found only as minor and rare transcripts in humans (*AMELX*), mice, rats, guinea pigs, and cows. It has been proposed that exon 4 (42 bp) is duplicated from exon 5 (having the same size) and subjected to accumulating mutations during mammalian evolution (Sire *et al.*, 2012). Inclusion of the duplicated exon 4 seems not to improve protein function or is deleterious to enamel matrix formation, a major functional role of amelogenin. However, it has been suggested that some transcripts including exon 4 function as signaling molecules (Veis, 1989). There are 16 alternative splicing transcripts in murine *Amelx*, but the ratio and abundance of the different isoforms vary considerably during the course of development (Iacob and Veis, 2006). Therefore, transcripts including exon 4 may have an important functional role in a specific time and location.

Targeted disruption of the murine *Amelx* gene resulted in disorganized hypoplastic enamel resembling human X-linked hypoplastic AI (Gibson *et al.*, 2001). A more interesting finding was that there was a thin layer of mineralized enamel, even though it was only 10% the thickness of normal enamel and also lacked a prism pattern (in contrast to the prismatic structure of enamel crystallites in normal enamel). These results indicate that the amelogenins are not required for the initial enamel mineralization but rather essential for the proper formation and elongation of the enamel crystal. A simplified knock-in mouse model expressing only 1 major amelogenin (without exon 4: M180) recently exhibited enamel with normal function and architecture, but the enamel hardness was increased while the toughness was decreased (Snead *et al.*, 2011). Therefore, it seems that M180 is enough to achieve normal enamel thickness and ordered elongation of the enamel crystal, and minor transcripts may be necessary for the fine-tuning of the mechanical properties of enamel.

In this study, M194 transgenic mice resulted in a porous and aprismatic enamel with reduced thickness and mineralization. This is in contrast to the fact that transgenic mice overexpressing M180 had a relatively normal enamel phenotype (Gibson *et al.*, 2007). It is obvious from the results that the forced expression of M194 is deleterious to enamel matrix mineralization. The abnormal enamel structure, which is porous and aprismatic, is also observed in the SEM image of the proband deciduous molar. Any deciduous tooth from the affected male was not available, but it seemed that the enamel phenotype was more severe in the male compared to the affected female based on the clinical and radiologic investigations.

In summary, our data show that a single transitional nucleotide change causing synonymous change in the middle of the *AMELX* exon 4, which is almost always skipped during pre-mRNA splicing, causes an increased exon definition by the strengthening of SC35 binding and the weakening of ESS motif binding. A transgenic model was generated and characterized to show tooth enamel defects mimicking the AI phenotype. We have uncovered that an unusual alteration of the ratio and quantity of the developmentally conserved alternative splicing repertoire of *AMELX* induces defects in enamel matrix mineralization.

ACKNOWLEDGMENTS

We would like to thank all the family members for their cooperation. This work was supported by grants from the Bio & Medical Technology Development Program (2013037491), the Science Research Center to the Bone Metabolism Research Center (2008-0062614), and the Basic Science Research Program (2013R1A2A1A01007642) through the National Research Foundation of Korea. The authors declare no potential conflicts of interest with respect to the authorship and/or publication of this article.

REFERENCES

Cho SH, Seymen F, Lee KE, Lee SK, Kweon YS, Kim KJ, *et al*. (2012). Novel FAM20A mutations in hypoplastic amelogenesis imperfecta. *Hum Mutat* 33:91-94.

Chun YH, Lu Y, Hu Y, Krebsbach PH, Yamada Y, Hu JC, *et al*. (2010). Transgenic rescue of enamel phenotype in Ambn null mice. *J Dent Res* 89:1414-1420.

Desmet FO, Hamroun D, Lalande M, Collod-Beroud G, Claustres M, Beroud C (2009). Human splicing finder: an online bioinformatics tool to predict splicing signals. *Nucleic Acids Res* 37:e67.

El-Sayed W, Parry DA, Shore RC, Ahmed M, Jafri H, Rashid Y, *et al*. (2009). Mutations in the beta propeller WDR72 cause autosomal-recessive hypomaturation amelogenesis imperfecta. *Am J Hum Genet* 85:699-705.

Gibson CW (1999). Regulation of amelogenin gene expression. *Crit Rev Eukaryot Gene Expr* 9:45-57.

Gibson CW, Yuan ZA, Hall B, Longenecker G, Chen E, Thyagarajan T, *et al*. (2001). Amelogenin-deficient mice display an amelogenesis imperfecta phenotype. *J Biol Chem* 276:31871-31875.

Gibson CW, Yuan ZA, Li Y, Daly B, Suggs C, Aragon MA, *et al*. (2007). Transgenic mice that express normal and mutated amelogenins. *J Dent Res* 86:331-335.

Hart PS, Hart TC, Michalec MD, Ryu OH, Simmons D, Hong S, *et al*. (2004). Mutation in kallikrein 4 causes autosomal recessive hypomaturation amelogenesis imperfecta. *J Med Genet* 41:545-549.

Iacob S, Veis A (2006). Identification of temporal and spatial expression patterns of amelogenin isoforms during mouse molar development. *Eur J Oral Sci* 114(Suppl 1):194-200.

Kang HY, Seymen F, Lee SK, Yildirim M, Tuna EB, Patir A, *et al*. (2009). Candidate gene strategy reveals ENAM mutations. *J Dent Res* 88:266-269.

Kim JW, Simmer JP, Hu YY, Lin BP, Boyd C, Wright JT, *et al*. (2004). Amelogenin p.M1T and p.W4S mutations underlying hypoplastic X-linked amelogenesis imperfecta. *J Dent Res* 83:378-383.

Kim JW, Seymen F, Lin BP, Kiziltan B, Gencay K, Simmer JP, *et al*. (2005a). ENAM mutations in autosomal-dominant amelogenesis imperfecta. *J Dent Res* 84:278-282.

Kim JW, Simmer JP, Hart TC, Hart PS, Ramaswami MD, Bartlett JD, *et al*. (2005b). MMP-20 mutation in autosomal recessive pigmented hypomaturation amelogenesis imperfecta. *J Med Genet* 42:271-275.

Kim JW, Simmer JP, Lin BP, Seymen F, Bartlett JD, Hu JC (2006). Mutational analysis of candidate genes in 24 amelogenesis imperfecta families. *Eur J Oral Sci* 114(Suppl 1):3-12; discussion 39-41, 379.

Kim JW, Lee SK, Lee ZH, Park JC, Lee KE, Lee MH, *et al*. (2008). FAM83H mutations in families with autosomal-dominant hypocalcified amelogenesis imperfecta. *Am J Hum Genet* 82:489-494.

Kim JW, Seymen F, Lee KE, Ko J, Yildirim M, Tuna EB, *et al*. (2013). LAMB3 Mutations Causing Autosomal-dominant Amelogenesis Imperfecta. *J Dent Res* 92:899-904.

Lee SK, Seymen F, Lee KE, Kang HY, Yildirim M, Tuna EB, *et al*. (2010). Novel WDR72 mutation and cytoplasmic localization. *J Dent Res* 89:1378-1382.

O'Sullivan J, Bitu CC, Daly SB, Urquhart JE, Barron MJ, Bhaskar SS, *et al*. (2011). Whole-Exome sequencing identifies FAM20A mutations as a cause of amelogenesis imperfecta and gingival hyperplasia syndrome. *Am J Hum Genet* 88:616-620.

Parry DA, Brookes SJ, Logan CV, Poulter JA, El-Sayed W, Al-Bahlani S, *et al*. (2012). Mutations in C4orf26, encoding a peptide with in vitro hydroxyapatite crystal nucleation and growth activity, cause amelogenesis imperfecta. *Am J Hum Genet* 91:565-571.

Parry DA, Poulter JA, Logan CV, Brookes SJ, Jafri H, Ferguson CH, *et al*. (2013). Identification of mutations in SLC24A4, encoding a potassium-dependent sodium/calcium exchanger, as a cause of amelogenesis imperfecta. *Am J Hum Genet* 92:307-312.

Poulter JA, Brookes SJ, Shore RC, Smith CE, Abi Farraj L, Kirkham J, *et al*. (2014a). A missense mutation in ITGB6 causes pitted hypomineralized amelogenesis imperfecta. *Hum Mol Genet* 23:2189-2197.

Poulter JA, El-Sayed W, Shore RC, Kirkham J, Inglehearn CF, Mighell AJ (2014b). Whole-exome sequencing, without prior linkage, identifies a mutation in LAMB3 as a cause of dominant hypoplastic amelogenesis imperfecta. *Eur J Hum Genet* 22:132-135.

Salido EC, Yen PH, Koprivnikar K, Yu LC, Shapiro LJ (1992). The human enamel protein gene amelogenin is expressed from both the X and the Y chromosomes. *Am J Hum Genet* 50:303-316.

Sauna ZE, Kimchi-Sarfaty C (2011). Understanding the contribution of synonymous mutations to human disease. *Nat Rev Genet* 12:683-691.

Sire JY, Huang Y, Li W, Delgado S, Goldberg M, Denbesten PK (2012). Evolutionary story of mammalian-specific amelogenin exons 4, "4b," 8, and 9. *J Dent Res* 91:84-89.

Snead ML, Zhu DH, Lei Y, Luo W, Bringas PO Jr, Sucov HM, *et al*. (2011). A simplified genetic design for mammalian enamel. *Biomaterials* 32:3151-3157.

Thesleff I (1995). Differentiation of ameloblasts and its regulation of epithelial-mesenchymal interactions. In: *Dental enamel: formation to destruction*. Robinson C, Kirkham J, Shore R, editors. Boca Raton, FL: CRC Press, p. 272.

Veis A (1989). Studies of vertebrate tooth mineralization. Insights from studies of dentinogenesis imperfecta type II. *Northwest Dent Res* 1:3-5.

Wang SK, Choi M, Richardson AS, Reid BM, Lin BP, Wang SJ, *et al*. (2014). ITGB6 loss-of-function mutations cause autosomal recessive amelogenesis imperfecta. *Hum Mol Genet* 23:2157-2163.

Witkop CJ Jr (1988). Amelogenesis imperfecta, dentinogenesis imperfecta and dentin dysplasia revisited: problems in classification. *J Oral Pathol* 17:547-553.